

Control of Cleavage Cycles in *Drosophila* Embryos by *frühstart*

Jörg Großhans,^{1,2,*} H. Arno J. Müller,³
and Eric Wieschaus²

¹ZMBH

Universität Heidelberg
Im Neuenheimer Feld 282
69120 Heidelberg
Germany

²Howard Hughes Medical Institute
Department of Molecular Biology
Princeton University
Princeton, New Jersey 08540

³Institut für Genetik
Heinrich-Heine-Universität
Universitätsstrasse 1, Geb. 26.02
40225 Düsseldorf
Germany

Summary

Early metazoan development consists of cleavage stages characterized by rapid cell cycles that successively divide the fertilized egg. The cell cycle oscillator pauses when the ratio of DNA and cytoplasm (N/C) reaches a threshold characteristic for the species. This pause requires maternal factors as well as zygotic expression of as yet unknown genes. Here we isolate the zygotic gene *frühstart* of *Drosophila* and show that it is involved in pausing the cleavage cell cycle. *frs* is expressed immediately after the last cleavage division. It plays a role in generating a uniform pause and it can inhibit cleavage divisions when precociously expressed. Furthermore, the expression of *frs* is delayed in haploid embryos and requires activity of the maternal checkpoint gene *grapes*. We propose that zygotic *frs* expression is involved in linking the N/C and the pause of cleavage cycle.

Introduction

Development in animal embryos begins with the cleavage stage, during which the large fertilized egg cell is split into increasingly smaller cells by an invariant number of rapid cell divisions. The end of cleavage and the associated transition to the following developmental stage is marked by a pause in the cell cycle, changes in cellular morphology, and a requirement for zygotic gene expression. This “midblastula transition” has been characterized in a variety of different animal species (e.g., *Xenopus*, zebrafish, *Drosophila*) and can be regarded as a simple example of a switch in developmental programs (Newport and Kirschner, 1982).

A common feature observed in many species is the control of the number of cleavage divisions by the nucleocytoplasmic ratio (N/C). The cleavage cell cycle pauses when the ratio of the amounts of DNA to cytoplasm reaches a specific threshold. In haploid embryos,

for example, there is one more cleavage division than in diploids; in tetraploid embryos there is one fewer (Boveri, 1902). According to a model discussed by Newport and Kirschner (1982), chromosomes titrate a cytoplasmic factor that represses the transition until its level reaches a critical value. The molecular nature of this control mechanism remains largely unclear, but the rate-limiting cytoplasmic factor apparently controls DNA replication, perhaps through some cell cycle component or checkpoint (Edgar and Datar, 1996; Sibon et al., 1997, 1999; Kimelman et al., 1987).

The entry of *Drosophila* embryos into cycle 14 and the following stage, cellularization, show many similarities to the midblastula transition observed in other species. *Drosophila* embryos have a superficial cleavage typical for insects with 13 nuclear divisions. In the last three cycles, mitotic cyclins (Edgar et al., 1994) and String/Twine, the Cdc25 phosphatases for Cdk1 in *Drosophila* (Edgar and Datar, 1996), may become limiting. The cell cycle lengthens from 8 to 18 min (Foe et al., 1993), and major zygotic transcription begins. The pause of the cleavage cell cycle that occurs in cycle 14 normally coincides with the onset of cellularization, a major morphological transition requiring genes like *nullo*, *bnk*, *slam*, and *sry- α* , whose transcription begins during the extended cycles and peaks by the end of cycle 13 (Schweisguth et al., 1990; Rose and Wieschaus, 1992; Scheijter and Wieschaus, 1993; Lecuit et al., 2002).

Cell cycle progression during the final cleavage divisions is monitored by a DNA repair checkpoint involving the protein kinase Grapes (D-Chk1) and Mei41 (Fogarty et al., 1997; Sibon et al., 1997, 1999; Yu et al., 2000). In one model, the checkpoint would delay mitosis in the last three cycles until DNA replication is completed, possibly by phosphorylating D-Cdc25, as suggested by the homology to Chk1 (Walworth et al., 1993; Sanchez et al., 1997). Embryos from *grapes* mutant females lack this checkpoint. Cell cycles 11–13 do not elongate, and perhaps as a consequence of incomplete DNA replication, the chromosomes arrest in metaphase 13. Other aspects of the cell cycle, like spindle formation and nuclear envelope breakdown and assembly, continue to undergo oscillations despite the metaphase arrest of the chromosomes, suggesting that the *grapes* checkpoint is required for the absolute pause in cell cycle characteristic of cycle 14. The pause may also involve an effect of *grapes* on zygotic transcription. Studies using α -amanitin indicate that at least some product of zygotic transcription is required for a complete cell cycle pause in cycle 14 (Gutzeit, 1980; Edgar et al., 1986; Edgar and Datar, 1996; Foe et al., 1993; Sibon et al., 1997). Although cycle 13 embryos mutant for *grapes* express the cellularization genes *nullo*, *slam*, and *bnk* (data not shown) and patterning genes *runt* and *ftz* (Sibon et al., 1997), the block in metaphase 13 appears to prevent the major increase in zygotic transcription that normally occurs in cycle 14 (Sibon et al., 1997). If the zygotic products required for the cell cycle pause normally accumulate only in cycle 14, the metaphase arrest in *grapes* might block their expression. On the other

*Correspondence: j.grosshans@zmbh.uni-heidelberg.de

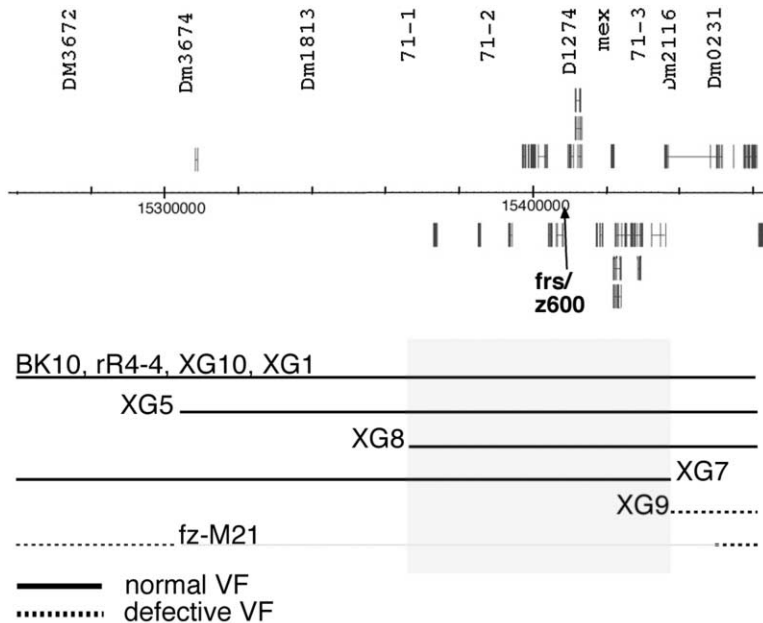


Figure 1. Mapping of *frs*
Physical map of the *frs/71CD* region with STS positions, the annotated genomic sequence according to Flybase, and the approximate breakpoints of the deficiencies. The lines of the deficiencies indicate the deleted region. The deficiencies Df(3L)XG9 and Df(3L)fz-M21 do not, while the other deficiencies indicated do, uncover the ventral furrow defect of *frs* when crossed to C(3) females.

hand, no such zygotic genes that are targets of *grapes* and control cell cycle progression have been identified.

In a previous study we and others investigated the interaction of mitosis and morphogenetic movements during ventral furrow formation and the invagination of the mesoderm anlage (Mata et al., 2000; Seher and Leptin, 2000; Großhans and Wieschaus, 2000). We described a mitotic inhibitor which specifically delays mitosis in the cells of the ventral furrow to prevent an interference of mitosis and furrow formation. At least two genes constitute the mitotic inhibitor: *tribbles* (*trbl*), encoding a protein kinase-related protein, and *frühstart* (*frs*).

Here we isolate the zygotic gene *frs*. In addition to its role during mesoderm invagination, *frs* appears to be involved in pausing the rapid nuclear cycles prior to cellularization. Since the onset of *frs* expression is delayed in haploid embryos with respect to the number of cleavage cycles, *frs* provides a link of the N/C and cleavage cell cycle pause.

Results

frs Encodes a Uniformly Expressed Small Basic Protein

Our initial approach to the cloning of *frs* relied on its cell cycle effects during gastrulation. We mapped the ventral furrow phenotype (Großhans and Wieschaus, 2000; Seher and Leptin, 2000) with deficiency chromosomes to a region of about 50 kb predicted to encode 18 transcripts (Adams et al., 2000; Figure 1). One of these transcripts (designated z600 by Schulz and Miksch, 1989) was described as having an expression profile reminiscent to that of *trbl*. To test whether this transcript encodes *frs*, we recombined a *frs* deficiency with a transgene carrying 1.7 kb of genomic DNA of this region. When crossed to C(3)se females, the deficiency alone produces a premature mitosis in all zgotically mutant embryos (104%; Table 1). The defect was eliminated by the transgene; the majority of the deficiency embryos

had a normal timing of mitosis and formed a proper ventral furrow, suggesting that we identified the *frs* gene (18%; Table 1).

frs encodes a cytoplasmic protein (see below) of 90 amino acid residues, including 19 basic residues with an isoelectric point of 10 (Schulz and Miksch, 1989). Proteins that have obvious similarities to the *frs* protein have not yet been described in any other species. We generated antibodies to the *frs* protein and confirmed their specificity by showing that they fail to stain *frs*-deficient embryos (Figures 2I–2L). On a cellular level, Frs appears to be excluded from the nucleus, despite its positive charge and a size below the apparent exclusion limit of the nuclear pores. When analyzed by immunofluorescence at higher resolution, Frs staining appears particulate (Figures 2 and 5; data not shown).

In wild-type embryos, *frs* RNA is expressed in a narrow peak early in cycle 14 (Figures 2A–2C) and is downregulated in a complex pattern during late cellularization and gastrulation. *frs* RNA persists until stage 9 (extended germband stages) in a set of dorsal cells, presumably the aminoserosa anlage (Figure 2D). Frs protein shows the same developmental profile (Figures 2E–2H). In *frs* mutant gastrula, only the cells of mitotic domain 10 divide prematurely. To test whether this spatially restricted phenotype is due to the pattern of *frs* expression during gastrulation, we uniformly expressed the *frs* cDNA in *frs*-deficient embryos under UAS control during cellularization and gastrulation (Table 1). Expression of the UAS-*frs* transgene rescued the mitotic defect in the ventral cells, but did not obviously delay mitosis in the other regions of the gastrula (Table 1), suggesting that differential sensitivity of the ventral furrow cells during gastrulation reflects a regional cell-type-specific restriction in *frs* activity.

frs Expression Is Sufficient to Pause the Cleavage Cycles

During gastrulation, *frs* inhibits mitosis in the ventral furrow. The stage when *frs* is first expressed, however,

Table 1. *frs* Phenotypes

(A) Ventral Furrow Phenotype			
Genotype/Cross	Normal VF	Defective VF	Penetrance (%)
Df <i>frs</i>	27	71	71
mGal4/UAS- <i>frs</i> ; Df <i>frs</i>	30	3	10
C(3) × Df <i>frs</i> /+	82	29	104 ^a
C(3) × <i>frs</i> ⁺ Df <i>frs</i> /+	165	8	18 ^a
(B) MBT Phenotype			
Genotype/Cross	13 Cycles (Normal)	14 Cycles (Partial, Comp.)	Penetrance (%)
Df <i>frs</i>	112	10	8
Df <i>frs</i> /+, +/+	304	1	0.3
4× <i>twn</i> ⁺	241	5	2
4× <i>twn</i> ⁺ ; <i>twn</i> ⁺ /+	211	36	15
4× <i>twn</i> ⁺ ; Df <i>frs</i>	12	88	88
4× <i>twn</i> ⁺ ; Df <i>frs</i> /+, +/+	180	70	28
4× <i>twn</i> ⁺ ; <i>frs</i> ⁺ Df <i>frs</i>	67	9	12
4× <i>twn</i> ⁺ ; <i>frs</i> ⁺ Df <i>frs</i> /+, +/+	143	18	11

(A) Embryos from mGal4; Df *frs*/TM3 females crossed with UAS-*frs*; Df *frs*/TM3 males scored for a premature mitosis (p-histone 3 staining) in mitotic domain 10. 25% of the embryos from the C(3) cross are homozygous for Df *frs*.

^aThe indicated penetrance is the actual score related to the expected 25%. mGal4, maternal Gal4; *frs*⁺, transgene with *frs* genomic region; VF, ventral furrow; temperature, 22°C.

(B) Extra nuclear division prior to cellularization (nuclear division 14). Embryos were stained, sorted according to their genotype and scored for an extra nuclear division, seen as randomly located patches of variable size. Less often, the extra division comprised the whole embryo. 4×*twn*⁺, homozygous second chromosome with a *twn*⁺ transgene; *frs*⁺, transgene with *frs* genomic region. Chromosome used: TM3, hb-lacZ, Df *frs*, Df(3L)BK10; temperature, 25°C.

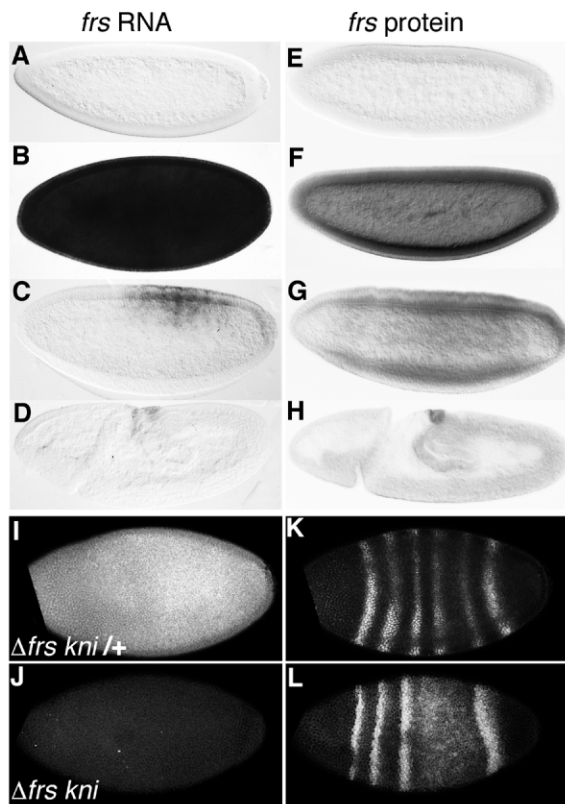


Figure 2. Expression of *frs*

frs detected in fixed wild-type embryos by RNA in situ hybridization (A–D) and by immunohistochemistry (E–H) ([A, B, E, and F], blastoderm; [C and G], gastrulation; [D and H], extended germband). Specificity of the *frs* antibody (I–L). *frs* homozygous (I and K), marked by *kni* and heterozygous embryos (J and L) stained for Frs (I and J) and Eve (K and L). The label $\Delta frs kni$ indicates the chromosome Df(3L)XG10 *kni*.

coincides with the more general pause in mitosis associated with the end of cleavage and the onset of cycle 14. To test whether Frs could also inhibit cleavage stage mitoses and thus might be involved in pausing the cell cycle in the cycle 14, we expressed *frs* prematurely by injecting synthetic *frs* mRNA into the posterior end of the embryos during cycles 10 to 12.

We found that posteriorly injected *frs* mRNA inhibited mitosis in most of the embryos (35 of 43 embryos scored; Figures 3C and 3D). In fixed embryos, patches with fewer and larger nuclei could be seen at the posterior injection site. The anterior regions of such embryos displayed a nuclear density normally observed in cycle 14. Injection of an unrelated mRNA, used as a control, did not change the mitotic behavior (*pelle* mRNA, 40 embryos scored). The premature end of cleavage resulted in a temporal asymmetry of cellularization. With live or fixed specimens or embryos carrying a histone 2Av-GFP, we observed that the cells at the injection site started cellularization prematurely, were more advanced during the process of cellularization, and also entered gastrulation before the surrounding cells (Figure 3D; data not shown). Cleavage divisions could also be stopped before cycle 12, when higher amounts of RNA were applied or injected before pole cell formation. These embryos did not enter cellularization. Instead, the nuclei stopped dividing and developed an abnormal morphology (data not shown). Such an early arrest prior to zygotic transcription would suggest that *frs* is sufficient for the cell cycle pause without any other zygotic factor.

It has been proposed that *stg* RNA is degraded by a zygotic factor (Edgar and Datar, 1996). To test whether *frs* may induce *stg* RNA degradation and consequently mitotic inhibition, we analyzed embryos that were locally injected with *frs* mRNA by *stg* RNA in situ hybridization (Figures 3H and 3I). We expect any direct effect of *frs* on *stg* RNA stability to be graded around the injection site, with the regions of mitotic inhibition corresponding

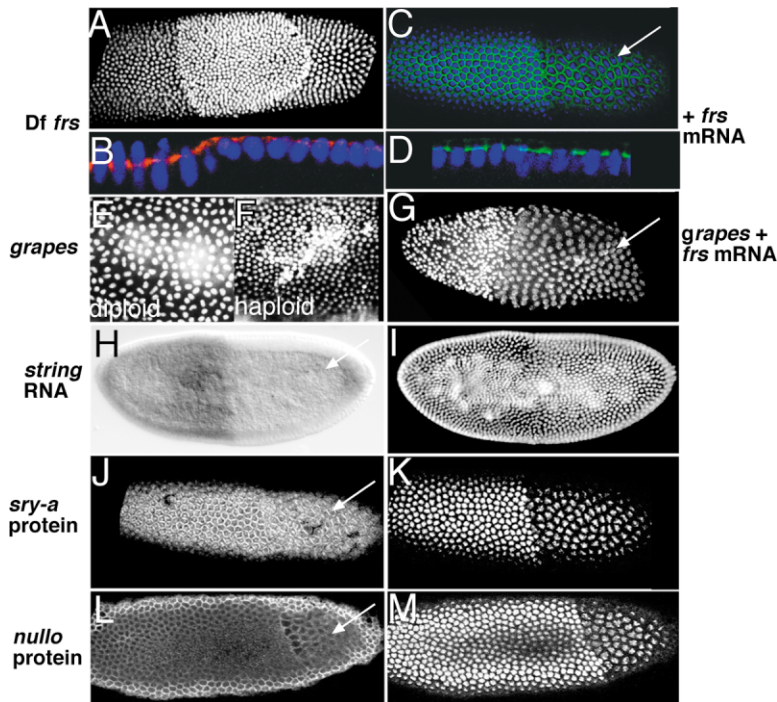


Figure 3. Control of Cleavage Cell Cycle by *frs*

(A and B) *Df frs* embryo [Df(3L)BK10] with a patch of higher nuclear density and asynchronous cellularization; DNA, blue; myosin, red.

(C, D, and G–M) Embryos injected with *frs* mRNA at the posterior side.

(C and D) Wild-type embryo; f-actin, green; DNA, blue.

(E and G) Diploid and (F) haploid ($x ms(3)K81$ males) embryos from *grapes* females.

(G) The nuclei in the posterior half lag behind by two cycles. Injected embryos stained for (H and I) *stg* RNA, (J and K) Sry- α protein, and (L and M) Nullo protein.

(A, E–G, I, K, and M) Fluorescent DNA staining. (C, J, and K) Photographs of the same embryo. (B and D) Cross-section at a higher magnification.

(E, F, H, and I) DIC and fluorescence optics. (A–D, G, and J–M) Optical sections (confocal optics).

to areas of maximal *stg* RNA degradation. We do in fact observe a reduction in *stg* RNA level in regions of lower nuclear density, but rather than being graded, the downregulation of *stg* RNA shows a sharp border that precisely matches the region of differential cell cycle behavior ($n = 16$). This observation suggests that the premature degradation of *stg* RNA may not be a direct consequence of injected *frs* activity, but instead a consequence of the pause in the cell cycle.

frs Is Involved in a Uniform Pause of the Cleavage Cycles

Given that *frs* is expressed immediately after the last cleavage division and injection of *frs* mRNA is sufficient to prematurely pause the cleavage cycles, we tested embryos for a previously undetected requirement of *frs* in the cycle 14 pause in mitosis. Among embryos deficient for *frs*, we observed a small fraction (less than 10%) containing patches of higher nuclear density which appear to be due to an extra (14th) cleavage division prior to cellularization (Figures 3A and 3B; Table 1). These patches are variable in size and location and in few cases comprise all cells of an embryo. In wild-type embryos such patches are not observed. Doubling the maternal dose of *twine* ($4 \times twn^+$), which by itself gives rise to an additional mitosis in a small proportion of the embryos (Edgar and Datar, 1996; Table 1), enhances the penetrance of the *frs* phenotype to almost 90% (Table 1). To test whether the extra mitosis is caused by absence of *frs* rather than by the other genes deleted in the deficiency chromosome, embryos homozygous for the *frs* deficiency carrying a *frs* genomic transgene were scored. In most of these embryos, the number of cleavage divisions was restored to 13 (88% to 12% penetrance for the $4 \times twn$ females; Table 1), suggesting that the absence of *frs* is responsible for the extra mitosis in

deficiency embryos. Furthermore, we injected *frs* dsRNA into wild-type embryos to mimic the effect of the deficiency and observed phenocopies in about 10% of the embryos (16/141; control RNAi, 0/140).

The consequence of the patchy extra cleavage cycle for embryogenesis is a temporal asymmetry of cellularization, formally similar to the asynchrony observed following *frs* mRNA injection. The nuclei/cells that divided only 13 times are more advanced than the nuclei that went through an additional mitosis (Figure 3B). During cellularization, the nuclei lengthen, and the furrow canal, which forms the tip of the invaginating plasma membrane, migrates basally. The cells that underwent additional divisions enter gastrulation later.

frs Expression Is Delayed in Haploid Embryos

The number of cleavage cycles is ultimately determined by the N/C, which appears to be facilitated in part by zygotic genes, because embryos treated with α -amanitin or embryos lacking the 3L chromosome arm undergo an extra cleavage division prior to cellularization like haploid embryos (Edgar et al., 1986; Merrill et al., 1988; Yasuda et al., 1991). Since *frs* is involved in pausing the cleavage cycle, we wondered whether *frs* expression might respond to the N/C.

First we analyzed the expression profile of *frs* RNA in diploid embryos during early development in greater detail. *frs* RNA is not expressed before mitosis 13 (Figures 2A and 4A; Table 2). Of 62 embryos in cycle 13, only two had a faint staining. The expression starts in mitosis 13, when the majority of the embryos displays weak staining (36 of 50). Full expression is observed immediately after completion of mitosis 13 (Figure 4B). The expression at the beginning of the cell cycle 14 is unusual. Other zygotic genes like *nullo*, *sry- α* , *hunchback*, and *slam* show a strong increase in the second

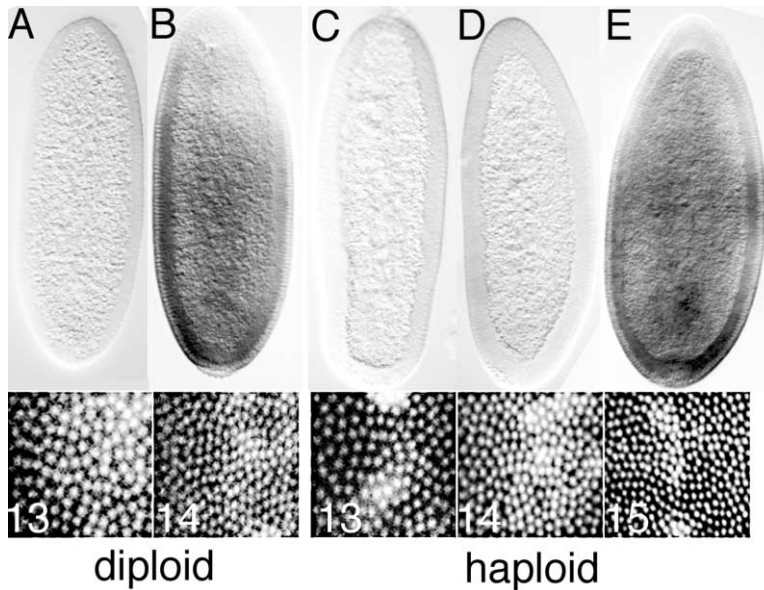


Figure 4. Expression of *frs* RNA in Haploid Embryos

frs RNA detected by in situ hybridization in diploid (A and B) and haploid (C–E) embryos from *fs(1)mh* females. The embryos were staged according to the nuclear density by the fluorescent DNA staining shown in the panels below each photograph: (A and C) no, (D) faint/weak, and (E) strong staining, classification of Table 2.

half of the interphase 13 immediately before entry into mitosis (data not shown).

Since the RNA detection method that we employed does not allow a more quantitative analysis of the expression levels, we established the expression profile for the *frs* protein using immunofluorescence staining. The age of the embryos was determined by the density of the nuclei and during cellularization by the distance between the basal end of the nuclei and the outline of the embryo. This distance is a linear function (with 0.2–0.3 $\mu\text{m}/\text{min}$) of the age of the embryos during cellularization (Figure 5I). Integrating the fluorescence signal provides a (nonlinear) measure for the expression level in individual embryos. As an internal control, the embryos were costained for *Sry- α* , which is expressed similarly to *Frs*, but independently of the N/C (Figure 5; Rose and Wieschaus, 1992). The *sry- α* transcript is slightly longer than the *frs* transcript, and neither gene has introns. The *frs* protein is not expressed during the cleavage cycles, including cycle 13, but becomes detectable within minutes after completion of mitosis 13 (Figures 5A, 5B, and 5J). The expression peaks after 15–30 min of cellularization as judged by nuclear length (Figures 5C, 5D, and

5J). The period of time between the last mitosis and the peak of *Frs* expression is in the range of the length of the preceding cleavage cycle and corresponds to the point in cycle 14 when an ectopic mitosis occurs in *frs* mutants or in haploid embryos (see below).

We then analyzed *frs* expression in haploid embryos. *frs* RNA is strongly expressed only in cycle 15, after the 14th nuclear division (Figures 4C–4E; Table 2; 136 of 154). No staining was observed in embryos in mitosis 13, and during interphase 14, mostly weak expression was observed (41 of 99, 5 with strong expression; Figure 4D). Comparing the profiles in diploids and haploids indicates a delay in haploid embryos with respect to the cell cycle number. Similarly *frs* protein is barely detectable and does not accumulate during the approximately 14 min of interphase 14 (Figures 5E and 5F). In cycle 15, however, *Frs* is detected in a profile comparable to cycle 14 in diploids (Figures 5G, 5H, and 5K). We found that *Sry- α* is expressed in cycle 14 of haploids and diploids in comparable levels (Figures 5E and 5F). In cycle 15 of haploids, *Sry- α* is present from the beginning of the interphase, while *Frs* shows a profile comparable to the cycle 14 profile in diploid embryos, reaching the high point of expression after about 15–30 min (Figures 5G, 5H, and 5K). Since *frs* RNA and protein expression is repressed in cycle 14 of haploid embryos and shifted to cycle 15, it appears that the onset of *frs* expression responds to the N/C.

Table 2. Expression Profile of *frs* RNA

Cycle Number	Diploid			Haploid		
	+++	+-	-	+++	+-	-
12	0	0	25	0	0	21
13	0	2	62	0	0	31
M13	0	36	14	0	0	9
14	237	42	11	2	27	43
M14				3	14	10
15				136	14	4

Diploid and haploid embryos were stained for *frs* RNA by in situ hybridization and scored for the number of divisions by their nuclear density and the intensity of the staining. +++, clear staining; +-, faint staining; -, no staining (see Figure 4D). Cycle 14 of the diploid and cycle 15 of the haploid embryos include only embryos in the first phase of cellularization before the nuclei have elongated. M13, M14, mitosis.

Relation of the Cell Cycle Pause and Zygotic Gene Expression

Cellularization immediately begins after the pause of the cell cycle, even when occurring one cycle too early. This connection suggests that the pause of the cell cycle and the start of zygotic transcription and cellularization are coordinated (Edgar and Schubiger, 1986). Alternatively, the cell cycle may be dominant over the various molecular rearrangements constituting this morphological transition. Since cellularization requires the expression of the zygotic genome, we ask whether there is a

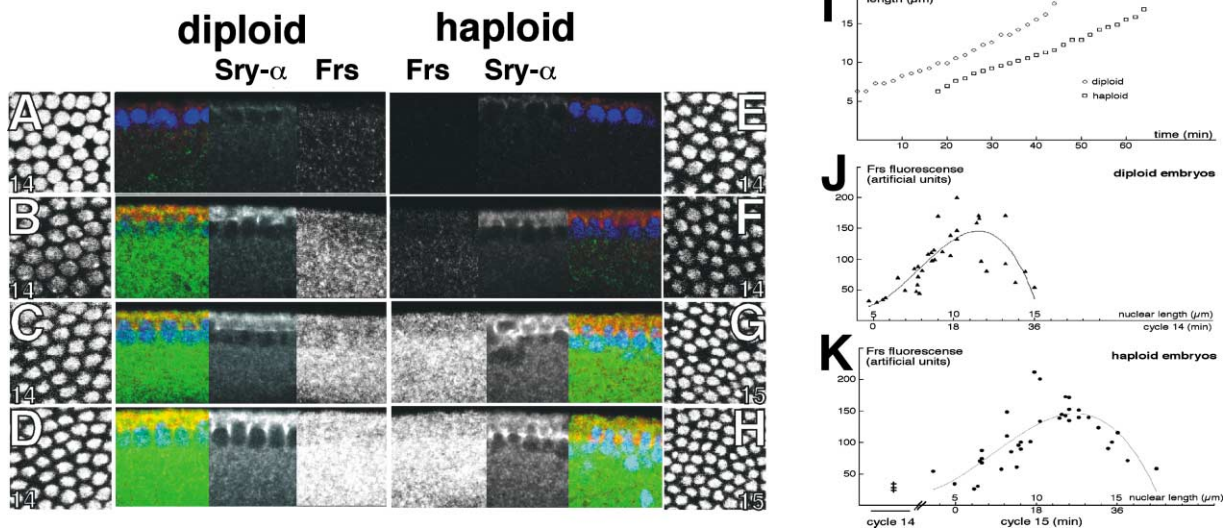


Figure 5. Expression of *frs* and *sry-α* Protein in Diploid and Haploid Embryos

(A–D) Diploid, cycle 14, (E and F) haploid, cycle 14, and (G and H) haploid, cycle 15. Nuclear density by DNA stain (surface view). The sections show the single channels for *Sry-α* and *Frs* and the overlay (red, *Sry-α*; green, *Frs*; blue, DNA). The invaginating membrane and length of the nuclei indicate how far cellularization has advanced.

(I) The distance between the basal end of the nuclei and the outline of the embryo as a function of time after mitosis 13 (cycle 14 in diploid, circles; cycle 15 in haploid, squares). The onset of cellularization in the haploid embryo was set to $t = 18$ min.

(J and K) Fluorescence of *Frs* staining in diploid (J) and haploid (K) embryos. Abscissa: age of the embryo in length and position of the nuclei (in μm) and the corresponding time in cycle 14 (J) or 15 ([K], in min). Ordinate: relative fluorescence of *Frs* staining in individual embryos. The abscissa in (K) is shifted by 18 min to take into account the extra cleavage cycle in haploid embryos. Crosses in (K) indicate the indirect *Frs* fluorescence of four haploid embryos in cycle 14. The fitted curves are cubic polynomial. The fluorescence intensity may be a nonlinear but monotonic function of *Frs* concentration. The absolute numbers of (J) and (K) cannot be compared.

correlation between the pause of the cell cycle and the onset of zygotic transcription of the cellularization genes *nullo* and *sry-α*. In a previous study, Rose and Wieschaus (1992) found that the onset of *nullo* and *sry-α* expression is similar in haploid and diploid embryos. Here we analyze whether the onset of expression is changed by a premature cell cycle pause. We stained embryos injected with *frs* mRNA for *Sry-α* or *Nullo* proteins (Figures 3J–3M). In all of the injected embryos with a premature transition in the posterior part (*Sry-α*, $n = 11$; *Nullo*, $n = 15$), *Sry-α* and *Nullo* staining appeared uniform with no obvious differences between anterior and posterior sides, suggesting that the onset of *sry-α* and *nullo* expression does not depend on the state of the cleavage cell cycle, at least during the cycles 13–14. These observations are in contrast with the differential degradation of maternal *stg* RNA in *frs* mRNA-injected embryos (Figures 3H and 3I) and suggests that the expression of *nullo* and *sry-α* may be controlled differently than the degradation of maternal *string* RNA.

The apparent cell cycle independence of *nullo* and *sry-α* expression is consistent with the earlier observation by Edgar et al. (1986) that the morphological events of cellularization, which require zygotic gene expression, are not delayed in haploid embryos. We repeated these studies using molecular markers for junction formation and membrane invagination (Hunter and Wieschaus, 2000). Both haploid and diploid embryos show a redistribution of cell surface Armadillo and myosin into adjacent nonoverlapping domains at the beginning of cycle 14 (Figure 6). This redistribution marks

the formation of the basal junction/furrow canal and indicates that both embryos initiate cellularization. In haploid embryos, this pattern is lost during the extra mitosis, but is restored at the onset of cycle 15 (Figures 6E–6H). This transient formation and reformation of the furrow canal in haploid embryos has also been observed in living embryos by time-lapse microscopy (Edgar et al., 1986; data not shown). Since these early morphological changes are initiated at cycle 14 in diploid and haploid embryos, we conclude that neither the morphological changes themselves nor the expression of genes that control them are dependent on the N/C that controls *frs* expression.

Correlation of *frs* and the *grapes* Checkpoint

In *Drosophila*, one well developed model for the cell cycle pause at cycle 14 invokes the DNA replication checkpoint controlled by the Chk1/Rad27 homolog *grapes*. This checkpoint is thought to extend interphase length in the last three cleavage cycles and then to pause the cleavage cycle after the 13th division (Fogarty et al., 1994, 1997; Sibon et al. 1997). Since *frs* is normally only transcribed after entry into cycle 14, the metaphase arrest in cycle 13 of *grapes* embryos would be expected to prevent *frs* expression. We have confirmed that this is the case, using RNA in situ hybridization of embryos from *grapes* females and observed little or no *frs* expression compared to wild-type embryos (data not shown). The effects of *grapes* are complex and clearly detectable before the mitosis 13 arrest (Su et al., 1999). Since the early effects of the *grapes* checkpoint have an impact

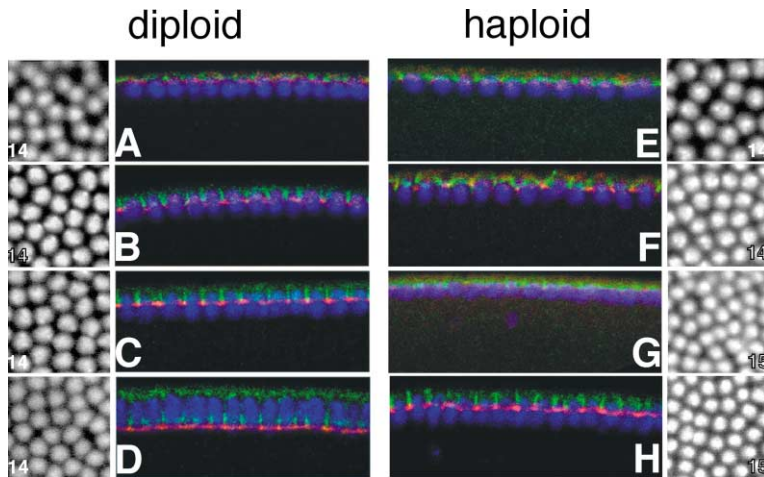


Figure 6. Cell Morphological Changes in Diploid and Haploid Embryos

Optical sections of fixed diploid (A–D) and haploid (E–H) embryos in cycle 14 (A–F) and 15 (G–H) labeled for DNA (blue), Myosin (red), and Armadillo (green). The nuclear cycle (14 or 15) was determined by the nuclear density seen in the surface view (DNA, white). Myosin marks the tip of the invaginating plasma membrane, and Armadillo marks the basal junction located apical to the furrow canal.

on the interpretation of *frs* role in the MBT, we reexamine the role of *grapes* in detecting the N/C.

Using the metaphase arrest as a readout, we compared the *grapes* phenotype in diploid and haploid embryos. Haploid embryos were obtained from eggs of *fs(1)mh* females or eggs fertilized by *ms(3)K81* males. In diploid embryos from *grapes* females, we observe nuclear densities corresponding to cycle 13 and lower ($n = 9$ in cycle 13; Figure 3E), while haploid embryos from *grapes* females reached densities corresponding to cycle 14 (cycle 14: with *ms(3)K81*, $n = 12$; with *fs(1)mh*, $n = 8$; Figure 3F). The doubled nuclear density and the apparent arrest in metaphase 14 in haploids suggests that the number of cleavage cycles in *grapes* embryos still depends on the N/C ratio, even though these embryos lack the *grapes* checkpoint. Thus the N/C must affect some property of the egg for which *grapes* activity is not essential to respond to the N/C, although the presence of a *grapes*-dependent checkpoint determines the nature of the response (see Discussion).

We also tested whether the cell cycle arrest induced by precocious expression of *frs* depends on the *grapes* checkpoint. We deposited *frs* mRNA in the posterior regions of *grapes* embryos and analyzed nuclear densities during cleavage (Figure 3G). Nuclear densities at the posterior injection site were 2- or 4-fold lower than those at the anterior end of the egg, indicating that posterior nuclei were lagging behind by one or two cycles. Earlier injection lead to an even stronger difference. These observations suggest that *frs* acts formally downstream or in parallel to *grapes*. Although *frs* injection thus produces similar cell cycle pauses in wild-type and *grapes* embryos, there is one crucial difference. In *grapes* embryos, the region paused in the cell cycle did not show any sign of premature cellularization, and f-actin distribution did not rearrange into a hexagonal array (data not shown). Although *grapes* embryos would be expected to express the early transcripts like *nullo* and *sry- α* , the morphological transitions associated with cellularization may also require the cell cycle progression and entry into cycle 14 interphase governed by the *grapes* checkpoint. Once those transitions have been initiated in cycle 14, the checkpoint may be irrelevant, but *frs* is still required to prevent mitosis that would disrupt the progress of cellularization.

Discussion

Based on the phenotypes reported in this study, we believe the simplest explanation for the *frs* function is that it inhibits entry into mitosis in a stage- and developmental-specific fashion. We initially identified the gene based on its role during gastrulation, when it delays mitosis during mesoderm invagination (Großhans and Wieschaus, 2000; Seher and Leptin, 2000). Here we describe and characterize a second function of *frs* at the end of the cleavage divisions: controlling the cell cycle pause after precisely thirteen mitoses. Similar developmental transitions are found in many animal embryos and are often referred to as the midblastula transition. In all cases studied so far, the timing of this transition depends on the ratio of nuclei to cytoplasm (N/C) and is shifted one cycle in haploid embryos where the nuclear DNA content is half that of diploids. We show that *Drosophila* embryos undergo a similar although less penetrant extra mitosis in the absence of *frs* and show fewer divisions if *frs* is precociously expressed. Since *frs* is itself differentially regulated in haploids and diploids, it may provide a unique handle on the junction between the N/C and the cell cycle pause.

Frs differs from other known cell cycle regulators in that it is not an essential component for cell cycle progression. Rather, *Frs* modulates and adjusts cell proliferation to requirements of the developmental program. In the absence of *frs*, the embryo develops, and the normal cell cycle control is largely maintained. Due to the lack of coordination, however, the overall efficiency and robustness of the cleavage-cellularization transition and mesoderm invagination is affected. The invariance is also disrupted by changing the maternal gene copy number of cell cycle regulators like *string* and *twine* (Edgar and Datar, 1996; Table 1), creating a genetic background in which *frs* is required for the correct cell cycle pause with a penetrance of the mutant phenotype of 90%. During both cleavage divisions and ventral furrow formation, the D-Cdc25 (*stg* and *twine*) and *frs* and *trbl* form opposite poles in a subtle balance that determines mitotic progression. The invariance of the transition is probably based on multiple regulatory inputs, so that natural variation in a single regulator does not lead to dramatic defects.

The gastrulation defects that led to *frs*'s identification also uncovered a second gene, *tribbles*, which encodes a kinase-like protein with a mutant phenotype similar to *frs* (Großhans and Wieschaus, 2000; Seher and Leptin, 2000; Mata et al., 2000). *Trbl* may act in concert with *Frs* to pause the cleavage cell cycle after 13 divisions, since onset of *trbl* expression is comparable to the onset of *frs* expression, and injection of synthetic *trbl* mRNA also stops the cleavage cycle prematurely. Their mutant phenotypes during ventral furrow formation are indistinguishable, and the double mutant does not produce any stronger effects (Großhans and Wieschaus, 2000).

Expression of *frs* shows two striking features that contrast with the behavior of previously characterized genes zygotically active in early *Drosophila* development. First, the expression peak is very narrow and rises in the early part of the interphase 14, only after the last cleavage division. The levels of other early zygotic transcripts (*nullo*, *sry- α* , *bnk*, *slam*) show strong increases slightly earlier, during the extended interphase 13, such that their levels are already high at the beginning of cycle 14. Second, unlike *nullo* and *sry- α* , *frs* expression apparently responds to the N/C. This particular expression pattern, together with its antimitotic activity, suggests a unique role for *frs* linking the N/C and the number of the cleavage divisions.

In the current model for pausing the cleavage cycle, called here the checkpoint model (O'Farrell et al., 1989; Edgar et al., 1994; Sibon et al., 1999), the N/C is measured by a maternal factor that is rate-limiting for DNA replication and is titrated by the increasing amount of chromatin. A DNA replication checkpoint involving *Grapes* and *Mei41* delays entry into mitosis until replication is complete. As the maternal replication factor becomes limiting and DNA replication slows, the checkpoint extends the G2 phase of the last three cleavage cycles. During these cycles, zygotic transcripts can be made before the replication checkpoint is released, and they accumulate to high levels before the nuclei pass through the last cleavage division. In cycle 14, these zygotic genes trigger the cell morphological changes characteristic for cellularization and may also prevent entry into mitosis 14 even when cycle 14 replication has been completed. In the context of this model, *frs* transcription and *Frs*'s antimitotic activity may be part of the zygotic response to prevent the extra division in cycle 14.

Certain features of the *frs* transcription profile, however, are not easily explained by this model and strongly suggest that *frs* transcription depends on an N/C detection system that operates in parallel with the checkpoint. In the extended cycles 11–13, *frs* transcription is still repressed, even though it has no introns and is smaller than many of the genes that are transcribed during that period. The failure to activate *frs* expression may reflect the fact that *frs* is normally expressed only at the beginning of the cell cycle and might not be affected by a replication checkpoint that primarily extends G2. Some other feature of the N/C must explain why *frs* is transcribed at the beginning of cycle 14, but not at the beginning of the preceding cycles. The same feature may also explain the delay in *frs* transcription in haploid embryos, a delay not observed for other genes like *nullo*

or *sry- α* , whose transcription begins in the cycles extended by the *grapes*-dependent checkpoint.

To incorporate these observations we propose that the N/C affects cell cycle progression in two essentially independent ways. One pathway relies on the *grapes*-dependent checkpoint and includes the role for the checkpoint in the previous model. In this model, the exponentially increasing number of nuclei would titrate some factor necessary for DNA replication such that by cycle 13, the decreased levels of this factor would retard replication. Incompletely replicated DNA would activate the *grapes* checkpoint to prevent entry into mitosis before DNA replication is completed. Failure to activate this checkpoint in *grapes* mutants would result in metaphase arrest and block the cell's entry into cycle 14. Since *frs* is normally transcribed at the beginning of cycle 14, metaphase-arrested embryos would fail to transcribe *frs*. The residual cycling observed in nuclear membrane breakdown and spindle morphology might reflect this absence and *frs*'s normal role in insuring an absolute pause in cycle 14. In this view, the immediate readout of the N/C ratio is delayed DNA replication. Removal of the *grapes* checkpoint affects morphological consequences of the N/C, but does not block the ability of the embryo to measure the N/C per se. This would be consistent with our finding that *grapes* mutant embryos are still sensitive to the N/C and shift the final point of their arrest by one cycle in haploid embryos.

The checkpoint per se however does not address why *frs* transcription is repressed in cycles 11–13. Although zygotic transcription of genes like *nullo* and *sry- α* occurs simultaneously with the extended interphases induced by the *grapes* checkpoint, our results and those of others (Sibon et al., 1997, 1999) indicate that the extensions are not essential for their transcription. Expression of *nullo* and *sry- α* during cycle 13 appears to be normal in *grapes* mutants. *Grapes* mutants do block the major burst in transcription during cycle 14, but this can be attributed to the condensed state of the chromosomes in the metaphase arrest. Although *grapes* is essential for the embryo to get to a point where it can express *frs*, given that the checkpoint is normally released prior to entry into mitosis 13, it is hard to see how activation of *grapes* in cycle 13 would directly affect transcription of *frs* at the start of the cycle that follows. It is possible that some residual signal of a previously activated checkpoint might persist through mitosis, but since the checkpoint accounts for the elongation of the earlier cycles 11 and 12, a persistent checkpoint signal would not explain the exclusive activation on *frs* in cycle 14. The one thing that distinguishes cycle 14 from the preceding cycles is not the existence of a preceding checkpoint but the N/C itself. In the simplest view, the N/C would directly influence *frs* transcription, triggering a switch that distinguishes cycle 14 from the preceding cycles. In haploid embryos, *frs* expression occurs after the switch has been delayed by one cycle.

The most direct test of our model may involve an analysis of the *cis*-acting control regions of the *frs* gene itself. Such an analysis might identify elements responsible for its differential expression in haploids and diploids. Equally relevant for the understand of *frs* function would be a biochemical analysis of the molecular mechanism that accounts for its antimitotic activity and how

the conserved cell cycle machinery is inhibited by this protein.

Experimental Procedures

Genetic Experiments

The *frs* gene is listed in flybase as Z600/CG17962 (Swissprot number P22469). Commonly used procedures, genetic material, and fly strains were applied and used as described in Lindsley and Zimm (1992), in the Flybase (<http://fly.ebi.ac.uk/>), and by the *Drosophila* Genome Project (BDGP, <http://www.fruitfly.org>). Staging of embryos was according to Campos-Ortega and Hartenstein (1997) or by the number of the cleavage cycle determined by the nuclear density. The following chromosomes and alleles were used: CyO, hb-lacZ, TM3, hb-lacZ, *kni*^{SG}, *fs(1)mh*, *ms(3)K81*, *mat-tubulin-GAL4* (St. Johnston, Cambridge), *His2AvGFP* (Yu et al., 2000), *string*^{TM5}, *string*^{AR2}, *grapes*^{ts1A4}, *C(3)se*, *Df(3L)BK10*, *Df(3L)rR4-4*, and *Df(3L)fz-M21*. *NulloHA*, *nullo* protein tagged with HA (hemagglutinin epitope) expressed by the *nullo* promoter (Hunter and Wieschaus, 2000). Insertions of a *twn*⁺ transgene on the second chromosome were obtained by mobilizing a *twn*⁺ genomic rescue construct with transposase (Alphay et al., 1992; Glover, Cambridge).

Characterization of the Genetic Region of *frs*

10⁴ males carrying a *w*⁺ insertion next to the *CrebA* gene (B204; Rose et al., 1997) were irradiated with X-rays. Out of 1.2 × 10⁵ mutagenized chromosomes in the F1 progeny, 42 *w* revertants were isolated, of which 17 are lethal over *Df(3L)BK10*. A genetic map was established with lethal mutations of the 71C–F region (collection of Cherbas, Bloomington) and other deficiencies. The physical map was established by PCR analysis with STS described in flybase (DM and mex primer pairs) and the following primer pairs: STS71-1 (TCCCAAGCCCCACTTTAAC, CCCCTTTGGGTGAATCTGC) maps between CG7804 and CG7489; STS71-2 (GCCCAACACGAAGTGTG TAC, GGTGCTAGAATGAAAAACAGCA, proximal to CG7815; and STS71-3 (GGATCCATCCTGGTGTCCC, CGCCATCCTCGATTACC) within CG17014. Homozygous embryos were identified by absence of the TM3, hb-lacZ balancer. Template DNA was obtained by boiling 5–10 embryos in 50–100 μl of water with a few chelex beads (Sigma). 0.1–0.5 embryo equivalents were used as templates for the PCR.

Mapping of *frs*

Embryos from crosses with *C(3)* females were scored for defective ventral furrow formation by live observation or staining of fixed embryos for mitotic nuclei (p-histone3).

Histology

Fixation (4% formaldehyde in PBS/heptane or boiling for 10 s) and protein and RNA detection in situ were performed according to common protocols. The following antibodies were used: anti-Arm (mouse clone N27A1, rabbit polyclonal, Wieschaus, Princeton, NJ), anti-Serendipity-α (mouse clone 6B12), anti-myosin (C. Fields, Boston, MA), anti-Eve (J. Reinitz, New York), anti-p-histone3 (Upstate), anti-β-galactosidase (Roche). RNA was detected with the Digoxigenin system with alkaline phosphatase (Roche). Proteins were detected by immunohistochemistry with peroxidase (Vector Lab, Burlington, VT) or by immunofluorescence with Alexa dyes (Molecular Probes). Filamentous actin was visualized with phalloidin coupled with fluorescent dyes (Molecular Probes). DNA was stained by Hoechst dye or oligreen (Molecular Probes). Specimens mounted in Durcupan (Fluka), Aquapolymount (Polysciences), or Mowiol/Dabco were observed with microscopes Zeiss Axioplan and Axiophot or Leica DMRXA (brightfield, differential interference contrast, fluorescence) and confocal microscopes Zeiss LSM510 and LeicaTCS. Photographs were taken on slide film (EPY64T, Kodak) or CCD cameras, digitalized, and enhanced with the computer program Photoshop (Adobe).

Frs Expression Profile

Frs expression was quantified with the computer program NIH Image (NIH, Bethesda, MD) by integrating the fluorescence (8 bit color depth) of *Frs* antibody staining in an area basally to the nuclei on the dorsal side at 50% egg length. The approximate age of the embryos in cellularization was determined by the distance between the outline of the embryo and the basal end of the nuclei. The fixation, staining, and evaluation of the diploid and haploid embryos

were performed in parallel, but in separate experiments, so that the absolute numbers cannot be directly compared. The parameters of the cubic polynomials were chosen by minimizing the sum of the square distances.

Molecular Genetics and Antibody Production

The *frs* cDNA was amplified by PCR with P1 clone DS08110 as template and primers JG70 (GGGAATTCAGTAGCAAATCAGCAACGTCA) and JG71 (GGCTCGAGAAGGCGCGGAAAGTAAATGT) and cloned as an EcoRI XhoI fragment into pCS2 (R. Rupp, Munich, Germany). The UAS-*frs* plasmid was made by transfer of *frs* cDNA from pCS-*frs* to pUAST. For the rescue experiment, the *frs* genomic region (–1205 to 468, +1 transcription start site) was amplified from P1 clone DS08110 by PCR (primer SV1, GGCTCGAGTACATGGTGGTGGGAGATG; SV8, GGATCGATAAGGCGCGGAAAGTAAATGT, with XhoI and ClaI sites), ligated to 3'HSP (cloned as a BamHI fragment from pCasperHS in pBKS), and transferred into the XhoI XbaI sites of pCasper4. *w* flies were transformed with pUAS-*frs* and p*Cfrs*-rescue by standard procedures (lines used: UAS-*frs*^D, *frs*⁺ [#1, III. chr.], *frs*⁺ [#19, II. chr.]). For production of recombinant protein, the *frs* coding sequence and 3'UTR were amplified with primers JG95 (GGGAATTCATGTCGTCGACCAATGAA) and JG71 and cloned as an EcoRI XhoI fragment into pGEX4T (Pharmacia). Serum (36/III) was obtained from rabbits immunized with recombinant GST-Frs expressed in *E. coli* and purified with GST-*frs* coupled to Sepharose (Pharmacia). The antibody was eluted with 4 M MgCl₂. dsRNA was prepared by transcription in vitro with T7 RNA polymerase (Roche, Mannheim). The templates for *frs* (full length) and CG9505 (500 bp; T. Lecuit, Marseille) were prepared by PCR with Taq DNA polymerase and included T7 promoter sites on both ends. Synthetic mRNA with a cap and a β-globin leader was synthesized as described (Großhans et al. 1999).

Microinjection of Embryos

Microinjection was performed as described (Großhans et al., 1999). mRNA and dsRNA were injected into the posterior half of stage 2–4 embryos at a concentration of 1 mg/ml, if not otherwise indicated. Injected embryos were fixed in 4% formaldehyde/PBS/Heptan. The vitelline membrane was manually removed.

Acknowledgments

We thank U. Abdu, S. Bartoszewski, B. Houchmandsade, T. Lecuit, T. Schüpbach, A. Swan, and the fly laboratories in Princeton and Heidelberg for discussions, suggestions, or comments on the manuscript. We gratefully received materials, reagents, or fly stocks from A. Carpenter, L. Cherbas, B. Edgar, C. Field, T. Lecuit, J. Reinitz, S. Smolik, F. Sprenger, D. St. Johnston, the *Drosophila* stock center (Bloomington, IN), and the Hybridoma bank in Iowa. We thank A. Baum and J. Goodhouse for assistance with microscopy, Y. Kussler-Schneider for technical assistance, S. Voltmer for cloning of the *frs* rescue construct, and A. Frank for DNA injections. J.G. thanks the fly laboratory in Tübingen for hospitality when having no U.S. visa. J.G. received a long-term fellowship from the Human Science Frontier Programme. This work is supported by the Emmy Noether program of the Deutsche Forschungsgemeinschaft, the Howard Hughes Medical Institute, and grant 5R37HD15587 from the NICHD.

Received: June 13, 2002

Revised: May 29, 2003

Accepted: May 29, 2003

Published: August 11, 2003

References

- Adams, M.D., Celniker, S.E., Holt, R.A., Evans, C.A., Gocayne, J.D., Amanatides, P.G., Scherer, S.E., Li, P.W., Hoskins, R.A., Galle, R.F., et al. (2000). The genome sequence of *Drosophila melanogaster*. *Science* 287, 2185–2195.
- Alphay, L., Jimenez, J., White-Cooper, H., Dawson, I., Nurse, P., and Glover, D.M. (1992). *twine*, a *cdc25* homolog that functions in the male and female germline of *Drosophila*. *Cell* 69, 977–988.
- Boveri, T. (1902). Ueber mehrpolige Mitosen als Mittel zur Analyse

- des Zellkerns. Verh. Mediz. phys. Gesellsch. Würzburg N. F. 35, 67–90.
- Campos-Ortega, J.A., and Hartenstein, V. (1997). The Embryonic Development of *Drosophila melanogaster*, 2nd Edition (Berlin, Heidelberg: Springer).
- Edgar, B.A., and Datar, S.A. (1996). Zygotic degradation of two maternal *cdc25* mRNAs terminates *Drosophila*'s early cell cycle program. *Genes Dev.* 10, 1966–1977.
- Edgar, B.A., Kiehle, C.P., and Schubiger, G. (1986). Cell cycle control by the nucleo-cytoplasmic ratio in early *Drosophila* development. *Cell* 44, 365–372.
- Edgar, B.A., and Schubiger, G. (1986). Parameters controlling transcriptional activation during early *Drosophila* development. *Cell* 44, 871–877.
- Edgar, B.A., Sprenger, F., Duronio, R.J., Leopold, P., and O'Farrell, P.H. (1994). Distinct molecular mechanisms regulate cell cycle timing at successive stages of *Drosophila* embryogenesis. *Genes Dev.* 8, 440–452.
- Foe, V.F., Odell, G.M., and Edgar, B.A. (1993). Mitosis and morphogenesis in the *Drosophila* embryo: point and counterpoint. In *The Development of Drosophila melanogaster*, M. Bate, and A. Martinez Arias, eds. (Cold Spring Harbor, NY: Cold Spring Harbor Laboratory Press), pp. 149–300.
- Fogarty, P., Kalpin, R.F., and Sullivan, W. (1994). The *Drosophila* maternal-effect mutation *grapes* causes a metaphase arrest at nuclear cycle 13. *Development* 120, 2131–2142.
- Fogarty, P., Campbell, S.D., Abu-Shumays, R., de Saint Phalle, B., Yu, K.R., Uy, G.L., Goldberg, M.L., and Sullivan, W. (1997). The *Drosophila* *grapes* gene is related to checkpoint gene *chk1/rad27* and is required for late syncytial division fidelity. *Curr. Biol.* 7, 418–426.
- Großhans, J., and Wieschaus, E. (2000). A genetic link between morphogenesis and cell division during formation of the ventral furrow in *Drosophila*. *Cell* 101, 523–531.
- Großhans, J., Schnorrer, F., and Nüsslein-Volhard, C. (1999). Oligomerisation of Tube and Pelle leads to nuclear localisation of Dorsal. *Mech. Dev.* 81, 127–138.
- Gutzzeit, H.O. (1980). Expression of the zygotic genome in blastoderm stage embryos of *Drosophila*: analysis of a specific protein. *Roux Arch. Dev. Biol.* 188, 153–156.
- Hunter, C., and Wieschaus, E. (2000). Regulated expression of *nullo* is required for the formation of distinct apical and basal adherens junctions in the *Drosophila* blastoderm. *J. Cell Biol.* 150, 391–401.
- Kimelman, D., Kirschner, M., and Scherson, T. (1987). The events of the midblastula transition in *Xenopus* are regulated by changes in the cell cycle. *Cell* 48, 399–407.
- Lecuit, T., Samanta, R., and Wieschaus, E. (2002). *slam* encodes a developmental regulator of polarized membrane growth during cleavage of the *Drosophila* embryo. *Dev. Cell* 2, 425–436.
- Lindsley, D.L., and Zimm, G.G. (1992). *The Genome of Drosophila melanogaster* (San Diego, CA: Academic Press).
- Mata, J., Curado, S., Ephrussi, A., and Rørth, P. (2000). Tribbles coordinates mitosis and morphogenesis in *Drosophila* by regulating String/CDC25 proteolysis. *Cell* 101, 511–522.
- Merrill, P. I., Sweeton, D., and Wieschaus, E. (1988). Requirements for autosomal gene activity during precellular stages of *Drosophila melanogaster*. *Development* 104, 495–509.
- Newport, J., and Kirschner, M. (1982). A major developmental transition in early *Xenopus* embryos: I. Characterization and timing of cellular changes at the mid-blastula stage. *Cell* 30, 675–686.
- O'Farrell, P.H., Edgar, B.A., Lakich, D., and Lehner, C.F. (1989). Directing cell division during development. *Science* 246, 635–640.
- Rose, L.S., and Wieschaus, E. (1992). The *Drosophila* cellularization gene *nullo* produces a blastoderm-specific transcript whose levels respond to the nucleocytoplasmic ratio. *Genes Dev.* 6, 1255–1268.
- Rose, E., Gallaher, N.M., Deborah, J.A., Goodman, R.H., and Smolik, S.M. (1997). The CRE binding protein dCREB-A is required for *Drosophila* embryonic development. *Genetics* 146, 595–606.
- Sanchez, Y., Wong, C., Thoma, R.S., Richman, R., Wu, Z., Piwnicka-Worms, H., and Elledge, S.J. (1997). Conservation of the Chk1 checkpoint pathway in mammals: linkage of DNA damage to Cdk regulation through Cdc25. *Science* 277, 1497–1501.
- Scheijter, E.D., and Wieschaus, E. (1993). *bottleneck* acts as a regulator of the microfilament network governing cellularisation of the *Drosophila* embryo. *Cell* 75, 373–385.
- Schulz, R.A., and Miksch, J.L. (1989). Dorsal expression of the *Drosophila* *z600* gene during early embryogenesis. *Dev. Biol.* 136, 211–221.
- Schweisguth, F., Lepesant, J.A., and Vincent, A. (1990). The serendipity alpha gene encodes a membrane-associated protein required for the cellularization of the *Drosophila* embryo. *Genes Dev.* 4, 922–931.
- Seher, T.C., and Leptin, M. (2000). Tribbles, a cell-cycle brake that coordinates proliferation and morphogenesis during *Drosophila* gastrulation. *Curr. Biol.* 10, 623–629.
- Sibon, O.C.M., Stevenson, V.A., and Theurkauf, W.E. (1997). DNA-replication checkpoint control at the *Drosophila* midblastula transition. *Nature* 388, 93–96.
- Sibon, O.C.M., Laurençon, A., Hawley, R.S., and Theurkauf, W.E. (1999). The *Drosophila* ATM homologue Mei-41 has an essential checkpoint function at the midblastula transition. *Curr. Biol.* 9, 302–312.
- Su, T.T., Campbell, S.D., and O'Farrell, P.H. (1999). *Drosophila* *grapes*/CHK1 mutants are defective in cyclin proteolysis and coordination of mitotic events. *Curr. Biol.* 9, 919–922.
- Walworth, N., Davey, S., and Beach, D. (1993). Fission yeast *chk1* protein kinase links the rad checkpoint pathway to *cdc2*. *Nature* 363, 368–372.
- Yasuda, G.K., Baker, J., and Schubiger, G. (1991). Temporal regulation of gene expression in the blastoderm *Drosophila* embryo. *Genes Dev.* 5, 1800–1812.
- Yu, K.R., Saint, R.B., and Sullivan, W. (2000). The *grapes* checkpoint coordinates nuclear envelope breakdown and chromosome condensation. *Nat. Cell Biol.* 2, 609–615.